

Design of an ultrafast electron diffractometer with multiple operation modes

Chun-Long Hu(胡春龙), Zhong Wang(王众), Yi-Jie Shi(石义杰), Chang Ye(叶昶), and Wen-Xi Liang(梁文锡)

Citation: Chin. Phys. B, 2021, 30 (**9**): 090701. DOI: 10.1088/1674-1056/ac11cd
Journal homepage: http://cpb.iphy.ac.cn; http://iopscience.iop.org/cpb

What follows is a list of articles you may be interested in

Effects of helium irradiation dose and temperature on the damage evolution of Ti_3SiC_2 ceramic

Hua-Hai Shen(申华海), Xia Xiang(向霞), Hai-Bin Zhang(张海斌), Xiao-Song Zhou(周晓松), Hong-Xiang Deng(邓洪祥), Xiao-Tao Zu(祖小涛)

Chin. Phys. B, 2019, 28 (**7**): 076104. DOI: 10.1088/1674-1056/28/7/076104

Ultrafast electron microscopy in material science

Huaixin Yang(杨槐馨), Shuaishuai Sun(孙帅帅), Ming Zhang(张明), Zhongwen Li(李中文), Zian Li(李子安), Peng Xu(徐鹏), Huanfang Tian(田焕芳), Jianqi Li(李建奇)

Chin. Phys. B, 2018, 27 (**7**): 070703. DOI: 10.1088/1674-1056/27/7/070703

Ultrafast electron diffraction

Xuan Wang(王瑄), Yutong Li(李玉同)

Chin. Phys. B, 2018, 27 (**7**): 076102. DOI: 10.1088/1674-1056/27/7/076102

Two-coupled structural modulations in charge-density-wave state of $SrPt_2As_2$ superconductor

Wang Li, Wang Zhen, Shi Hong-Long, Chen Zhen, Chiang Fu-Kuo, Tian Huan-Fang, Yang Huai-Xin, Fang Ai-Fang, Wang Nan-Lin, Li Jian-Qi

Chin. Phys. B, 2014, 23 (**8**): 086103. DOI: 10.1088/1674-1056/23/8/086103

Misfit-layered compound $PbTiS_3$ with incommensurate modulation：Transmission electron microscopy analysis and transport properties

Shen Xi, Cheng Dan, Zhao Hao-Fei, Yao Yuan, Liu Xiao-Yang, Yu Ri-Cheng

Chin. Phys. B, 2013, 22 (**11**): 116102. DOI: 10.1088/1674-1056/22/11/116102

Design of an ultrafast electron diffractometer with multiple operation modes*

Chun-Long Hu(胡春龙), Zhong Wang(王众), Yi-Jie Shi(石义杰), Chang Ye(叶昶), and Wen-Xi Liang(梁文锡)†

Wuhan National Laboratory for Optoelectronics (WNLO), Huazhong University of Science and Technology, Wuhan 430074, *China*

(Received 27 May 2021; revised manuscript received 26 June 2021; accepted manuscript online 7 July 2021)

Directly resolving structural changes in material on the atomic scales of time and space is desired in studies of many disciplines. Ultrafast electron diffraction (UED), which combines the temporal resolution of femtosecond-pulse laser and the spatial sensitivity of electron diffraction, is an advancing methodology serving such a goal. Here we present the design of a UED apparatus with multiple operation modes for observation of collective atomic motions in solid material of various morphologies. This multi-mode UED employs a pulsed electron beam with propagation trajectory of parallel and convergent incidences, and diffraction configurations of transmission and reflection, as well utilities of preparation and characterization of cleaned surface and adsorbates. We recorded the process of electron–phonon coupling in single crystal molybdenum ditelluride following excitation of femtosecond laser pulses, and diffraction patterns of polycrystalline graphite thin film under different settings of electron optics, to demonstrate the temporal characteristics and tunable probe spot of the built UED apparatus, respectively.

Keywords: ultrafast electron diffraction, electron optics, diffraction geometry, structural dynamics

PACS: 07.78.+s, 61.05.J–, 63.20.kd **DOI:** 10.1088/1674-1056/ac11cd

1. Introduction

Ultrafast electron diffraction[1–10] (UED) is a pump–probe approach using laser pulses to initiate and clock the process of dynamics under investigation,[11] and pulsed electron bunches with precisely controlled delay with regard to the pump laser to record the transient structure of specimen undergoing structural change. In a general UED setup, the electron pulse is generated through photoemission stimulated by a part of the pump laser pulse, usually frequency up-converted, duplicating the spatial and temporal profiles of the stimulation light. Although suffering the temporal degradation due to electron pulse-width broadening in propagation,[12–14] and velocity mismatch between the pump laser and the probe electron with relatively low kinetic energy,[5,13,14] UED provides resolutions in time domain of picosecond (ps) to femtosecond (fs) and in reciprocal space of sub-milli-ångström associated with electron diffraction, capable of resolving atomic structural changes on the ultrashort time-scale when such changes occur. Compared to the well established time-resolved x-ray diffraction with equivalent spatiotemporal resolutions,[15–19] UED has advantages of high scattering cross section of electron scattered by nuclei in matter, which enables the high sensitivity to surface and samples with low dimensionality, and low cost and compact setup, which allows for table-top design and integration with other techniques and instruments. UED has been the method of choice for studies of structural dynamics spanning in fields of physics, chemistry, and materials,[2–10,20–26] and made significant findings of transient molecular structure in reactions,[27] solid–liquid phase transition of metal melting,[28] changes of hydrogen bonding network in interfacial water,[29] bond dilation and metastable state in phase deformation of vanadium dioxide,[30,31] charge delocalization driven by molecular motions in organic salt,[32] short time scales of energy transfer across polymer–graphene heterostructures,[33] optical manipulation of phonon modes of solid during phase transition,[34] and many others.

Since the first UED setup was pioneered by Mourou *et al.*,[1,35] the methodology of UED advances majorly in two aspects during the past four decades. One aspect is to pursue better performance, mainly better temporal resolution for resolving faster dynamics, as the short wavelength nature of electron (1.23 Å for low kinetic energy of 100 eV and 0.02 Å for 300 keV) leads to no much demand for improvement of spatial resolution in the UED development. Along with the evolution of ultra-short pulse laser techniques, the implements of radio-frequency compression,[36–38] mega-eV electron source,[39–41] terahertz radiation compression,[42,43] and highly compact instrument design[44–47] make UED leap in temporal resolution from hundreds of ps to nowadays tens of fs.[48] On the other hand, efforts have been made to extend the capabilities of UED, *i.e.*, to apply UED in more fields. For example, UED working in reflection geometry[49] was applied in tracking transient structure of germanium surface[50] and phospholipids,[51] and thermal transport across

*Project supported by the Director Fund of WNLO (Grant No. WNLOZZYJ1501), the Fundamental Research Funds for the Central Universities, HUST (Grant No. 2017KFXKJC001), the Innovation Fund of WNLO, and the Fund of State Key Laboratory of Magnetic Resonance and Atomic and Molecular Physics (Grant No. T152012).

†Corresponding author. E-mail: wxliang@hust.edu.cn

© 2021 Chinese Physical Society and IOP Publishing Ltd

a heterostructure interface;[52] convergent-beam UED was employed to map out lattice deformations in silicon wedge[53,54] and graphite sheet;[55,56] pulsed electron sources working with medium kinetic energy of 1 keV–10 keV[45] and low kinetic energy of hundreds of electron volts[33,34,46,47] were designed to specify UED in studies of thin film, monolayer, surface, and interface.

In this contribution, we present the design of a UED apparatus aimed at working with multiple operation modes for the versatility of studies in a broad range of disciplines, by one integrated setup. This multi-mode UED (MMUED) is constructed with a chamber system designed for operations in both transmission and reflection geometries, a pulsed electron gun (e-gun) delivering parallel and convergent beams, and the integration of utilities for preparation and characterization of cleaned surface and adsorbates. The selections of the diffraction modes of transmission and reflection, and the incidence modes of parallel and convergent electron beam (e-beam), make MMUED applicable in probing samples of a wide variety of possible forms of bulk, thin film, surface, adsorbate, heterostructure, and nano-scale structure on substrate.

2. Design and setup

Like a typical UED apparatus, MMUED is configured with an ultra-high vacuum (UHV) chamber system, and devices of utility and function mounted on the ports. We exerted two specific designs to achieve multiple operation modes. One is the compact-designed chamber system, in which the architecture and port arrangement are suitable for diffraction in both transmission and reflection geometries, as well the assembly of utilities on the translation pathway of the manipulator for preparation and characterization of cleaned surface sample. The other is that the pulsed e-gun is assembled with a delicate set of electron-optical elements, in which the trajectories of emitted electrons are modulated to form desired probe spot and incident angle on the sample.

2.1. The overall design and the UHV chamber system

The overall design of MMUED is depicted in Fig. 1. The UHV chamber system is constructed with two major chambers, the diffraction chamber for time-resolved diffraction measurement and the preparation chamber for sample processing and characterization, connected in a tee-shape layout. Compared to the previously reported UED setup with an elbow-shape layout and relative large scale of dimension,[4] such a layout design eliminates the intermediate steps of passing sample stage between different transfer rods during sample transferring from the preparation chamber to the diffraction chamber, *i.e.*, a direct sample transfer between these two chambers. A direct transfer is critical to the preparation and investigation of temperature-dependent sample like crystalized ice.[29] A Ti:sapphire amplified laser system is used to provide MMUED with ~ 40 fs pulses centered at 800 nm in a repetition rate of 5 kHz. Each fs laser pulse is split into two parts, one part with the majority of energy is guided to the diffraction chamber to initiate dynamics under investigation, the other part with minor energy is frequency tripled to generate pulsed electrons from the e-gun. The relative arrival time on sample of pump laser pulse and probe electron pulse is controlled by a linear stage on the optical pathway, like other pump–probe setup.

In the diffraction chamber, the pulsed e-gun and a detector (not shown in Fig. 1) are mounted in-line for diffraction measurement. The detector with sensitivity to single-electron event consists of a phosphor screen-based UHV compatible detector (*e.g.*, a vacuum image detector from Photek Ltd) and a combo of image intensifier and charge-coupled device (CCD)/complementary metal–oxide semiconductor (CMOS) camera, or a microchannel plate based detector (usually with a cheveron configuration) and a CCD/CMOS camera, for better signal-to-noise ratio for experimental configurations of different wavelengths of pump light and kinetic energies of probe electron. Viewports are designed on the side and top of the chamber to pilot the pump laser. For measurements of transmission geometry, the pump beam goes through the side port, denoted by the blue arrow in Fig. 1, to illuminate the sample in a near-collinear incidence assisted by the steering mirror to reduce the velocity mismatch.[5,57] For measurements of reflection geometry, the pump beam goes through the top port, denoted by the red arrow in Fig. 1, to illuminate the sample perpendicularly to the e-beam pathway. The perpendicular geometry of the pump laser overlapping with the e-beam introduces a severe velocity mismatch, which requires a temporal compensation by tilted intensity distribution of the pump light,[58] see discussion in Subsection 2.3.

In the preparation chamber, the 5-axis (three degrees of freedom in translation and two axes of rotation for positioning the sample and searching for diffraction condition) goniometer for sample transfer and manipulation defines the layout of connected utilities. A load lock chamber and a sample storage chamber are designed to straddle the manipulator to protect the cleaned chambers and samples. Along the pathway of the manipulator, a wobble stick for sample handling under UHV condition, a combo of ion sputter gun and gas doser for cleaning/roughening surface and depositing adsorbate, a quadrupole mass spectrometry (QMS) for analysis of residual gas species in the chamber, and a combo of low energy electron diffraction (LEED) and Auger electron spectroscopy (AES) for calibration of surface crystallization and analysis of surface chemical residual, respectively, are in-line mounted on the top of the chamber, as illustrated in Fig. 1. Combined with the heating and cooling functions implemented in the go-

niometer, we are able to prepare and characterize samples with cleaned surface and adsorbate, then directly transfer the sample into the diffraction chamber for *in-situ* dynamics measurements.

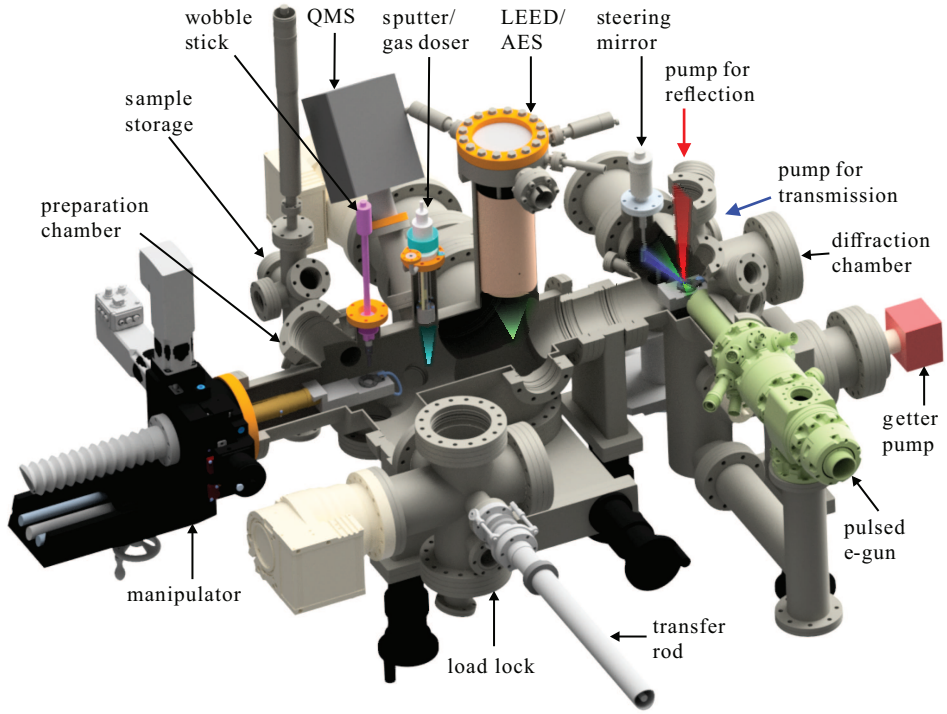


Fig. 1. Schematics of the MMUED apparatus and the section view of UHV chamber system. The pump laser beam for transmission configuration (blue arrow) is introduced through a side viewport of the diffraction chamber, then steered by a mirror for near-axis illumination on the sample, while the pump for reflection configuration (red arrow) is introduced through a top viewport for perpendicular illumination. The art shapes in color of cyan, green, blue, and red denote at where the particles of ion, electron, and photon interact with the sample in the preparation chamber and diffraction chamber.

2.2. Pulsed electron gun with parallel and convergent beam

We adopted features of electron optics from transmission electron microscopy to construct our pulsed e-gun, as schematically shown in Fig. 2, rendering a constitution more complex than the original design of UED derived from streak camera.[1] The lanthanum hexaboride (LaB_6) single crystal cathode with a diameter of 25 μm emits photoelectron bunches under stimulation of ultraviolet fs laser pulses, through front-illumination. The pulsed e-beam gains kinetic energy, maximum of 30 keV, by acceleration of the extraction field between the cathode and anode, then streams through the electron optics assembly of condenser lens, quadrupoles, aperture, octopoles, and objective lens, which work with electrostatic fields instead of magnetic ones, composing a magnetism free configuration. Both the condenser lens and objective lens may apply a maximum voltage of 20 kV. Regulating the voltages on two lenses modulates the emission from e-gun tunable between parallel beam and convergence beam, and focuses the e-beam with a spot size on the sample tunable from $\sim$ 100 μm to $\sim$ 10 μm. A tunable probe spot size benefits better diffraction signals from nonuniform samples, and enables change of diffraction feature as demonstrated in Section 3.

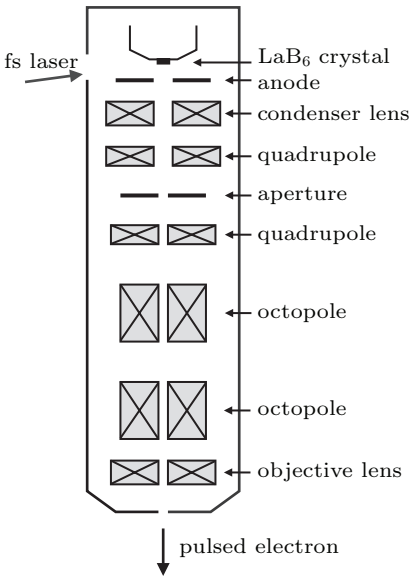


Fig. 2. Schematics of the pulsed e-gun with a complex electron optics assembly. A side viewport is designed to introduce stimulation light for generation of photoemission electrons from the LaB_6 photocathode. Two quadrupoles are designed to collimate the e-beam through downstream electron optics, and two octopoles are designed to reshape the e-beam profile.

Given that the temporal resolution of UED is set by the temporal width of pump laser pulse and electron pulse, and the temporal mismatch due to the velocity discrepancy between the two pulses,[5,14] our complex design of electron optics assembly is a trade-off between the desirable capability and the available temporal resolution. The temporal width of the elec-

tron pulse is mainly determined by the strength of extraction field and the length of travel pathway of electron pulse.[13,14] The temporal mismatch depends on the geometrical arrangement of the two pulses, and the probe area, *i.e.*, the footprint of the electron pulse impinging on the sample. We managed the pathway length in the e-gun column relatively short as $\sim$ 327 mm. Benefit from the two-lens design, a tight focusing of $\sim$ 100 μm spot diameter for parallel beam is achieved at the location of $\sim$ 50 mm away from the e-gun end. When the photoelectron emission is tuned to contain less than one thousand electrons per pulse, we estimate an overall temporal resolution of sub-picosecond in dynamics measurements for the built MMUED, which will be demonstrated in Section 3.

2.3. Multiple operation modes of MMUED

In Fig. 3 we illustrate typical applications of MMUED and the corresponding sample morphology and diffraction feature.

The most common use of UED is to probe samples in a transmission geometry with parallel incidence, as depicted in Figs. 3(a) and 3(b) for samples of polycrystal thin film and single crystal membrane, generating Debye–Scherer rings, and Bragg spots, respectively. Expanding the incidence angle enables UED to probe structural dynamics of single crystal bulk sample with a convergent beam generating Kikuchi bands or line pairs, as depicted in Fig. 3(c). The spanned wave vectors of convergent beam overcome the limitation of single incident wave vector of parallel beam, by an Ewald sphere with effective thickness in the reciprocal space to simultaneously map out more crystallographic directions of a unit cell. The nature of Kikuchi diffraction originated inside the region far away from sample surface, at where the diffused probe electrons are secondary scattered, brings higher spatial sensitivity in terms of detecting lattice deformations, compared to Bragg diffraction by parallel beam incidence,[53] rendering UED with convergent beam specific potentials in studies of dynamics of strain engineering or heat rectification.

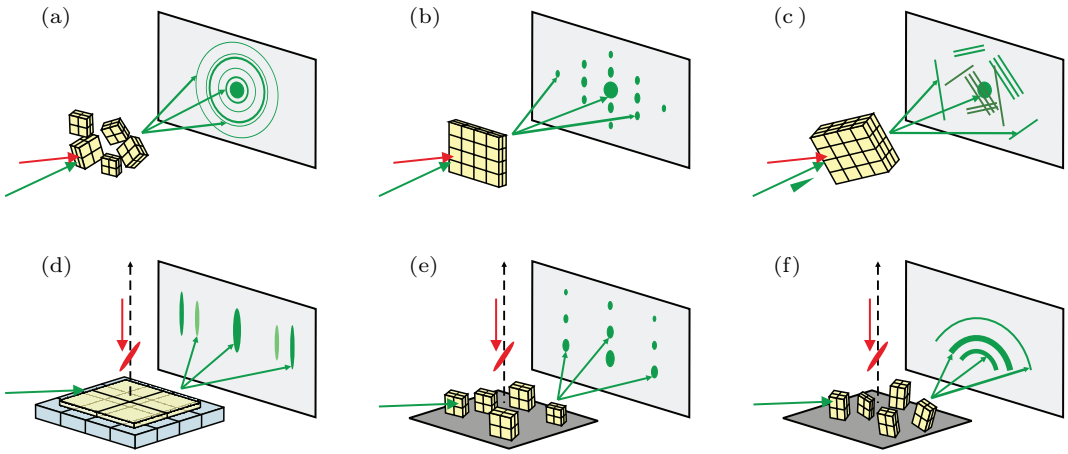


Fig. 3. Typical applications of MMUED and the corresponding sample morphology and diffraction feature. Red arrows and green arrows represent the pump laser beams and the probe e-beams, respectively. (a)–(c) Transmission configurations for samples of polycrystalline thin film, single crystal membrane, and single crystal bulk flake, respectively. The green triangle in panel (c) denotes the convergent e-beam impacting the sample. (d)–(f) Reflection configurations for samples of cleaned surface with adsorbate, orientated nano-crystallites on substrate, and randomly distributed nano-crystallites on substrate, respectively. The red ovals denote the tilted pump pulses, see text for details.

In a reflection geometry, UED is able to investigate samples with morphology not accessible to the transmission configuration. Samples in transmission configuration are mounted and orientated in a geometry that the normal of sample surface is parallel to the pathway of e-beam, so that the e-beam probes samples perpendicularly. To operate UED in reflection configuration, samples are mounted and orientated in a geometry that the sample surface is almost parallel to the pathway of e-beam, so that the e-beam probes samples with a grazing angle. In Fig. 3(d), the e-beam impacts the sample surface with a tangential incidence, generating diffraction relrods due to very shallow region probed. Accompanied with the utilities implemented in the preparation chamber, as discussed in Subsection 2.1, this operation mode makes MMUED suitable to monitor structural changes in a very localized region started from the sample surface, and the adsorbate on top of substrate surface.[59,60] In cases that samples are nano-crystalized structures grown on a substrate, the e-beam actually probes the region of interest with a transmission incidence, although the experimental setup is in a reflection configuration, as illustrated in Figs. 3(e) and 3(f) for crystallites with aligned orientation and random orientation, generating Bragg spots and Debye–Scherer rings, respectively. It is noted that only a half-set of the diffraction pattern is accessible to the detector in cases of Figs. 3(e) and 3(f) because of blocking by the substrate. In order to record high order diffraction features in reflection configuration, a wedge shaped flange is inserted between the e-gun and the diffraction chamber, so that the propagation pathway of e-beam deviates $\sim 1^\circ$ from the axis of detector, pointing the direct beam to the side area of the detector instead of

the center in transmission configuration. Another drawback of reflection configuration is that the grazing angle elongates the footprint on sample surface, causing a severe temporal degradation due to the effect of group velocity mismatch between electron and laser pulses, *e.g.*, a footprint of 30-keV electrons traveling in the speed of 0.33 c yields 10.1-ps/mm dispersion of time zero along the direction of e-beam pathway for a typical grazing angle of 1°. To overcome the degradation of velocity mismatch, a tilting scheme of pump laser is needed in reflection configurations to alter the intensity distribution of laser pulses, so that the sample is excited precisely at the same time regards to the arrival of electrons at the probed area.[56,61]

3. Demonstrations of experimental result

In this section we demonstrate the temporal characteristics, the tunable size of probe spot, and patterns in reflection configuration of the built MMUED apparatus. Figure 4(a) shows the initial change of diffraction feature of 1T′ molybdenum ditelluride ($MoTe_2$) upon excitation of femtosecond laser with 1028-nm wavelength and ∼ 200-fs pulse duration. The sample is a mechanically peeled membrane of single crystal. As depicted in Fig. 4(a), the peak height averaged over the (020) Bragg spot rapidly decreases as a function of delay time between excitation pulses and electron pulses, yielding a time constant of 1.1 ps by a mono-exponential fit. The rapid change of Bragg spot is indicative to the ultrafast process of electrons coupling their extra energy gained from excitation photons to phonons in $MoTe_2$. More details of the study will be reported elsewhere.

In Figs. 4(b) and 4(c), the static diffraction patterns recorded by pulsed electrons change as the probe spot sizes are changed by the modulation of electron optics. The sample is a polycrystalline graphene film with few layers. When a voltage of 7 kV is applied to the objective lens, the size of e-beam spot is large enough to cover adequate graphene grains to form Debye–Scherer rings in Fig. 4(b). When the voltage applied to the objective lens is 9 kV, two sets of Bragg spot from the same sample area probed in Fig. 4(b) are clearly formed in Fig. 4(c), indicating the shrunken e-beam spot covers only a few grains. The tunable e-beam spot size provides possible distinction of phases of heterostructure sample with different grain sizes.

Figures 4(d) and 4(e) show diffraction streaks from a sapphire surface by MMUED in reflection configuration. Rotations in polar and azimuthal axes provide precise alignments for diffraction conditions in reflection mode. In Fig. 4(e), another crystallographic direction comes into the in-phase condition compared to the pattern in Fig. 4(d), when the sample is slightly rotated.

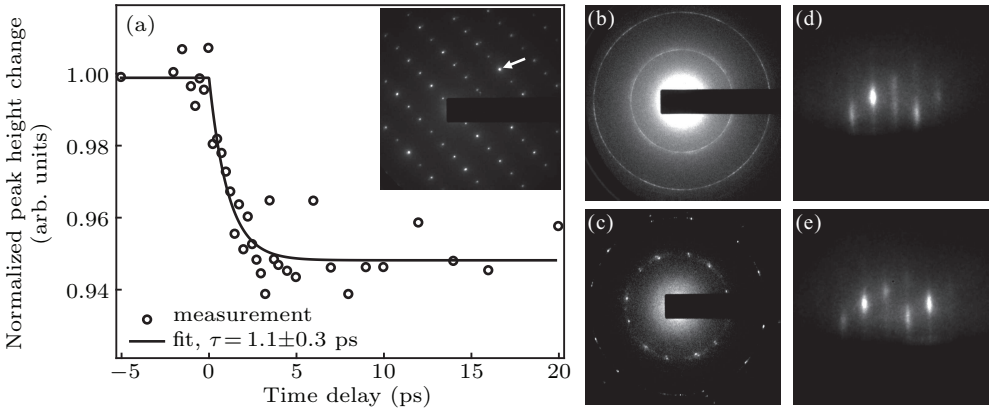


Fig. 4. Ultrafast change of Bragg spot of 1T′ $MoTe_2$, diffraction feature changes of patterns in transmission mode for polycrystalline graphene thin film and reflection mode for surface of single crystal sapphire. (a) The normalized peak height change of (020) Bragg spot (marked by the white arrow in the inset) of $MoTe_2$ follows excitation of femtosecond laser pulses, indicating a rapid process of electron–phonon coupling. Inset: Diffraction pattern of 1T′ $MoTe_2$ single crystal. (b) Debye–Scherer rings are formed through adequate amount of graphene grains probed by the e-beam spot with large size. (c) Bragg spots are formed through a few graphene grains when the e-beam spot shrinks. (d) and (e) Different crystallographic directions come into the in-phase diffraction condition in reflection mode.

4. Conclusion

We reported a design of UED apparatus with multiple operation modes for observations of ultrafast structural dynamics in solid materials of a wide range of morphologies covering bulk, thin film, surface, adsorbate, heterostructure, and nanostructure on substrate. The desired capabilities are achieved by implementations of the pulsed e-gun with delicate electron optics and the compact UHV chamber system optimized for both transmission and reflection diffraction geometries and integration of utilities for surface preparation. The versatility and the chosen low kinetic energy of e-beam make MMUED specifically suitable for investigations of emerging material family for energy harvest, conversion, and storage, which are developed in various morphologies and structures for diverse device strategies, and are often vulnerable to radiation of electrons with high kinetic energy. We anticipate MMUED addressing the transient state and the interplay between electron subsystem and phonon/lattice subsystem of materials, from the structural degrees of freedom, in study of many topics.

Acknowledgments

We thank Mr. Jiufeng Jia, Ms. Yun Liu, Ms. Renwen Cui, Ms. Yali Wang, Dr. Qun Li, Mr. Haowen Zhou and Ms. Bingxue Wang for their contributions to setting up the MMUED apparatus, and Mr. Tyler Ruttan for his helpful discussions during the design of pulsed e-gun.

References

[1] Mourou G and Williamson S 1982 *Appl. Phys. Lett.* **41** 44
[2] Dantus M, Kim S B, Williamson J C and Zewail A H 1994 *J. Phys. Chem.* **98** 2782
[3] Zewail A H 2005 *Phil. Trans. R. Soc. A* **363** 315
[4] Yang D S, Gedik N and Zewail A H 2007 *J. Phys. Chem. C* **111** 4889
[5] Nie S, Wang X, Li J, Clinite R and Cao J 2009 *Microsc. Res. Tech.* **72** 131
[6] Ruan C Y, Murooka Y, Raman R K, Murdick R A, Worhatch R J and Pell A 2009 *Microsc. Microanal.* **15** 323
[7] Miller R J D, Ernstorfer R, Harb M, Gao M, Hebeisen C T, Jean-Ruel H, Lu C, Moriena G and Sciaini G 2010 *Acta Cryst.* A**66** 137
[8] Sciaini G and Miller R J D 2011 *Rep. Prog. Phys.* **74** 096101
[9] Yang J, Guehr M, Vecchione T *et al*. 2016 *Faraday Discuss.* **194** 563
[10] Ischenko A A, Weber P M, Miller R J D 2017 *Chem. Rev.* **117** 11066
[11] Williamson J C, Cao J, Ihee H, Frey H and Zewail A H 1997 *Nature* **386** 159
[12] Qian B L and Elsayed-Ali H E 2002 *J. Appl. Phys.* **91** 462
[13] Siwick B J, Dwyer J R, Jordan R E and Miller R J D 2002 *J. Appl. Phys.* **92** 1643
[14] Srinivasan R, Lobastov V A, Ruan C Y and Zewail A H 2003 *Helv. Chim. Acta* **86** 1761
[15] Rousse A, Rischel C and Gauthier J C 2001 *Rev. Mod. Phys.* **73** 17
[16] Pfeifer T, Spielmann C and Gerber G 2006 *Rep. Prog. Phys.* **69** 443
[17] Chergui M and Zewail A H 2009 *ChemPhysChem* **10** 28
[18] Kim J, Kim K H, Lee J H and Ihee H 2010 *Acta Cryst.* A**66** 270
[19] Miller R J D 2014 *Science* **343** 1108
[20] Williamson J C and Zewail A H 1994 *J. Phys. Chem.* **98** 2766
[21] Zewail A H 2000 *J. Phys. Chem. A* **104** 5660
[22] Dwyer J R, Hebeisen C T, Ernstorfer R, Harb M, Deyirmenjian V B, Jordan R E and Miller R J D 2006 *Phil. Trans. R. Soc. A* **364** 741
[23] Zewail A H 2006 *Ann. Rev. Phys. Chem.* **57** 65
[24] Zewail A H and Thomas J M 2009 *4D Electron Microscopy: Imaging in Space and Time* (London: Imperial College Press) pp. 200–258
[25] Miller R J D 2014 *Ann. Rev. Phys. Chem.* **65** 583
[26] Feist A, Storeck G, Schäfer S and Ropers C 2018 *MRS Bull.* **43** 504
[27] Ihee H, Lobastov V A, Gomez U M, Goodson B M, Srinivasan R, Ruan C Y and Zewail A H 2001 *Science* **291** 458
[28] Siwick B J, Dwyer J R, Jordan R E and Miller R J D 2003 *Science* **302** 1382
[29] Ruan C Y, Lobastov V A, Vigliotti F, Chen S and Zewail A H 2004 *Science* **304** 80
[30] Baum P, Yang D S and Zewail A H 2007 *Science* **318** 788
[31] Morrison V R, Chatelain R P, Tiwari K L, Hendaoui A, Bruhács A, Chaker M and Siwick B J 2014 *Science* **346** 445
[32] Gao M, Lu C, Jean-Ruel H, Liu L C, Marx A, Onda K, Koshihara S y, Nakano Y, Shao X, Hiramatsu T, Saito G, Yamochi H, Cooney R R, Moriena G, Sciaini G and Miller R J D 2013 *Nature* **496** 343
[33] Gulde M, Schweda S, Storeck G, Maiti M, Yu H K, Wodtke A M, Schäfer S and Ropers C 2014 *Science* **345** 200
[34] Horstmann J G, Böckmann H, Wit B, Kurtz F, Storeck G and Ropers C 2020 *Nature* **583** 232
[35] Williamson S, Mourou G and Li J C M 1984 *Phys. Rev. Lett.* **52** 2364
[36] Chatelain R P, Morrison V R, Godbout C and Siwick B J 2012 *Appl. Phys. Lett.* **101** 081901
[37] Mancini G F, Mansart B, Pagano S, van der Geer B, de Loos M and Carbone F 2012 *Nucl. Instrum. Methods Phys. Res. A* **691** 113
[38] Williams J, Zhou F, Sun T, Tao Z, Chang K, Makino K, Berz M, Duxbury P M and Ruan C Y 2017 *Struct. Dyn.* **4** 044035
[39] Li R, Huang W, Du Y, Yan L, Du Q, Shi J, Hua J, Chen H, Du T, Xu H and Tang C 2010 *Rev. Sci. Instrum.* **81** 036110
[40] Musumeci P, Moody J T, Scoby C M, Gutierrez M S and Westfall M 2010 *Appl. Phys. Lett.* **97** 063502
[41] Zhu P, Zhu Y, Hidaka Y, Wu L, Cao J, Berger H, Geck J, Kraus R, Pjerov S, Shen Y, Tobey R I, Hill J P and Wang X J 2015 *New J. Phys.* **17** 063004
[42] Kealhofer C, Schneider W, Ehberger D, Ryabov A, Krausz F and Baum P 2016 *Science* **352** 429
[43] Zhang Z, Yan L, Du Y, Zhou Z, Su X, Zheng L, Wang D, Tian Q, Wang W, Shi J, Chen H, Huang W, Gai W and Tang C 2016 *Phys. Rev. Lett.* **116** 184801
[44] Gerbig C, Senftleben A, Morgenstern S, Sarpe C and Baumert T 2015 *New J. Phys.* **17** 043050
[45] Badali D S, Gengler R Y N and Miller R J D 2016 *Struct. Dyn.* **3** 034302
[46] Storeck G, Vogelgesang S, Sivis M, Schäfer S and Ropers C 2017 *Struct. Dyn.* **4** 044024
[47] Vogelgesang S, Storeck G, Horstmann J G, Diekmann T, Sivis M, Schramm S, Rossnagel K, Schäfer S and Ropers C 2018 *Nat. Phys.* **14** 184
[48] Lu C, Jiang T, Liu S, Wang R, Zhao L, Zhu P, Xiang D and Zhang J 2018 *Phys. Rev. Lett.* **120** 044801
[49] Elsayed-Ali H E and Mourou G A 1988 *Appl. Phys. Lett.* **52** 103
[50] Zeng X, Lin B, El-Kholy I and Elsayed-Ali H E 1999 *Phys. Rev. B* **59** 14907
[51] Chen S, Seidel M T and Zewail A H 2006 *Angew. Chem. Int. Ed.* **45** 5154
[52] Gorfien M, Wang H, Chen L, Rahmani H, Yu J, Zhu P, Chen J, Wang X, Zhao J and Cao J 2020 *Struct. Dyn.* **7** 025101
[53] Yurtsever A and Zewail A H 2011 *Proc. Natl. Acad. Sci.* **108** 3152
[54] Yurtsever A, Schaefer S and Zewail A H 2012 *Nano Lett.* **12** 3772
[55] Liang W, Vanacore G M and Zewail A H 2014 *Proc. Natl. Acad. Sci.* **111** 5491
[56] Feist A, da Silva N R, Liang W, Ropers C and Schäfer S 2018 *Struct. Dyn.* **5** 014302
[57] Williamson J C and Zewail A H 1993 *Chem. Phys. Lett.* **209** 10
[58] Baum P and Zewail A H 2006 *Proc. Natl. Acad. Sci.* **103** 16105
[59] Schäfer S, Liang W and Zewail A H 2011 *J. Chem. Phys.* **135** 214201
[60] Liang W, Schäfer S and Zewail A H 2012 *Chem. Phys. Lett.* **542** 1
[61] Kreier D and Baum P 2012 *Opt. Lett.* **37** 2373